Chapter 4: Hypothesis of Diffusion-Limited Growth

Summary

This section derives a useful equation to predict quantum dot size evolution under typical organometallic synthesis conditions that are used to achieve narrow size distributions. Assuming diffusion-controlled growth before Ostwald ripening, organometallic synthesis kinetics should be characterized by an activation energy, *Q*. Traditionally, *Q* would be extracted from the slope in an Arrhenius plot of *ln*(rate) versus 1/*T*, where *T* is the absolute temperature. Recently, a study of CdSe quantum dots grown in stearic acid (SA) used Arrhenius analysis to estimate *Q* from molar growth rates.[68] It has also been demonstrated that *Q* can be estimated from photoluminescence (PL) redshift rates (*i.e.* the changes in PL peak wavelength per change in reaction time between sequential samples).[69]

The Problem

Peng clearly stated that the growth of CdSe quantum dots formed via organometallic synthesis should be limited by the diffusion of metal precursors, rather than by the surface reaction rate.[58] Almost all literature in this field offers evidence that supports this idea. Despite detailed theoretical treatments, we still lack reasonable analytical expressions for the mean radius versus time that are consistent with diffusion-limited growth in a batch process. Although diffusion generally exhibits Arrhenius

temperature dependence, diffusion activation energies have not been experimentally measured and published for nanocrystal synthesis in various solvents.

Therefore, the goal of this chapter is to develop analytical expressions, describing the evolution of nanocrystal radii as a function of time and temperature, in order to help estimate activation energies from experimental measurements.

Assumptions

Some simplifying assumptions may facilitate achieving a manageable expression for R versus t. I specifically *hypothesize* that the diffusion of precursors into a CdSe nanocrystal is reasonably approximated by a *linear* concentration gradient across a diffusion length, L_D, that should correspond to the effective ligand length when synthesis includes strong complexes of Cd with TOPO and with TDPA. To visualize how a linear concentration gradient might surround a quantum dot that was synthesized in stearic acid, Figure 4-1 uses a decreasing intensity of color to represent how the concentration of cadmium stearate molecules may decrease towards the surface, due to stearic hindrance from ligands attached to the CdSe nanocrystal.

To be explicit, the mathematical model is based on the following assumptions:

1. A fast reaction rate reduces the surface concentration of Cd complexes, C_{inter} (in moles cm^{-3}), to a level that is orders of magnitude lower than in the bulk fluid, so that $C_{inter} \sim 0$.

2. During the growth stage, the diffusion of Cd complexes is significantly slower than the diffusion of Se, so that the reduced supply of Cd is the rate-limiting step for CdSe nanocrystal growth.

3. The bulk reaction fluid outside of the diffusion boundary layer is well stirred to maintain a homogeneous concentration of Cd complexes, C_{bulk} (in moles cm^{-3}), which are gradually consumed with reaction time.

4. A diffusion barrier region of constant thickness, L_D, exists around the surface of each nanocrystal. If this barrier is assumed to be caused by ligands pacifying dangling bonds on the surface of the nanocrystal, then L_D may correspond to the hydrodynamic diameter or the effective length of the ligand. However, L_D could also represent a wider reactant depletion length in the reaction solvent.

5. The radial concentration gradient from $x = R$ to $x = L_D$ is approximately linear from the nanocrystal surface to the outside of the diffusion barrier; so the gradient is given by (4-1), where x is the radial distance from the center of the nanocrystal.

$$\left.\frac{dC}{dx}\right|_{x=R} \sim \frac{C_{bulk} - C_{interior}}{L_D} \sim \frac{C_{bulk}}{L_D} \tag{4-1}$$

6. Growth conditions are controlled to insure roughly spherical quantum dots, not rods, with a radius of $R_{(t)}$ (in cm), which increases with reaction time, so that the surface area, A, is given by (4-2).

$$A = 4\pi R^2 \tag{4-2}$$

7. Mobility of the Cd complex is limited by standard diffusion with Arrhenius temperature behavior, Equation (4-3). Then the diffusivity, D (in $cm^2\ s^{-1}$), is characterized by a diffusion activation energy, Q (in eV), and by a pre-exponential diffusivity coefficient, D_o (in $cm^2\ s^{-1}$), where k_b is Boltzman's constant, and T is the absolute temperature (in K). D_o does not depend on the Cd complex concentration.

$$D = D_o \exp\{-Q/k_bT\} \tag{4-3}$$

8. The model only simulates quantum dot growth after nucleation and before Ostwald ripening, and it assumes that the number of nuclei, *N*, remain constant during this period.[59]

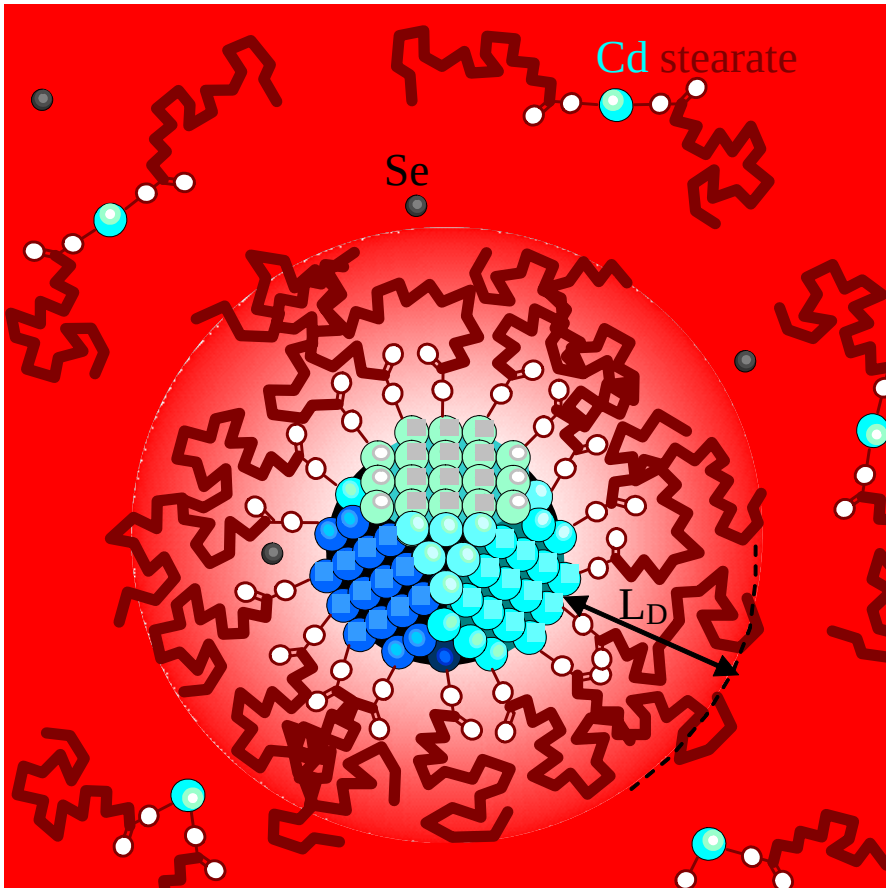

Figure 4-1. Diagram of a CdSe quantum dot growing in stearic acid. The illustration shows how the diffusion length, *L*, might represent the thickness of a ligand barrier.

Using the assumptions of linear concentration gradients (4-1), spherical nanocrystals (4-2), and Arrhenius diffusion (4-3), Fick's first law (4-4) yields a governing Equation (4-5) for the molar growth rate, *v*, where *J* is the flux of Cd into the nanocrystal (in moles cm^{-2} s^{-1}).

$$v = -A \cdot J = A\frac{dC}{dx}D \qquad (4\text{-}4)$$

$$v_{(t)} \approx 4\pi\, R_{(t)}^2 \frac{C_{bulk(t)}}{L_D} D_o \exp\left\{-\frac{Q}{k_b T}\right\} \tag{4-5}$$

Temporal Evolution of Nanocrystal Radius

Positive and negative feedback on the growth rate can be seen by expressing $v_{(t)}$, C_{bulk}, and R in terms of m, the total number of moles of precursor (4-6), where V_{org} (in cm^3) is the volume of all the organic material in the reaction. The molar volume of CdSe (V_m = 33.34 cm^3 $mole^{-1}$) is its molecular weight (W = 191.37 g $mole^{-1}$) divided by its density (ρ = 5.74 g cm^{-3}), based on unit cell volume.[64] Others[59] estimate V_m to be 32.995 cm^3 $mole^{-1}$. N_{eff} is the effective number of spherical nanocrystals that would contain the number of moles of Cd that have been consumed.

$$v = -\frac{1}{N_{eff}}\frac{dm}{dt}, \quad C_{bulk} = \frac{m}{V_{org}}, \quad \text{and} \quad R = m^{1/3}\left(\frac{3V_m}{4\pi N_{eff}}\right)^{1/3} \tag{4-6}$$

The governing Equation (4-5) becomes a simple differential Equation (4-7), with a coefficient, $\Theta_{(T)}$, which does not vary with time, but does depend on temperature. Integration from an intermediate time after nucleation, t_i, (when the remaining moles of precursor is m_i) to the reaction time, t, yields an expression (4-8) describing how m changes during the reaction.

$$\frac{dm}{dt} = -\Theta_{(T)}\, m^{1/3}, \qquad \text{where } \Theta_{(T)} \equiv \frac{4\pi D_o}{V_{org} L}\left(\frac{3V_m}{4\pi N_{eff}}\right)^{2/3} \exp\left\{-\frac{Q}{k_b T}\right\} \tag{4-7}$$

$$m_{(t)} = \left(m_i^{2/3} - (2/3)\Theta_{(T)}\{t - t_i\}\right)^{3/2} \tag{4-8}$$

It is helpful to express the differential Equation (4-7) and its solution (4-8) in unitless forms (4-10) and (4-11), respectively, by defining a remaining precursor fraction

f, an intermediate precursor fraction f_i (at t_i), and a reaction completion time t_c (4-9). Integrating (4-10) from an intermediate time t_i after nucleation to a given synthesis time t (in s) yields an expression (4-11) that describes how reactants are gradually depleted. The intermediate precursor fraction f_i is less than 1.0 because some reactants are consumed during nucleation.[58]

$$f \equiv \frac{m}{m_o} = \frac{C_{bulk(t)}}{C_{bulk(to)}}, \qquad f_i \equiv \frac{m_i}{m_o} = \frac{C_{bulk(ti)}}{C_{bulk(to)}}, \qquad \tau_c \equiv \frac{3(f_i m_i)^{2/3}}{2\Theta_{(T)}} \tag{4-9}$$

$$df/dt = -\Theta_{(T)}\, f^{1/3} \tag{4-10}$$

$$f_{(t)} = f_i\left(1 - \frac{\{t - t_i\}}{t_c}\right)^{3/2} \tag{4-11}$$

Growth of the average quantum dot radius (4-12) can be derived geometrically from (4-11) and (4-6), where C_o is the original molar concentration of Cd in the batch (in moles cm^{-3}). Using Equation (2-6), the wavelength of the first absorbance peak λ_{abs} can be estimated from the average radius according to (4-13), where $X = 0.82 \times 10^{-7}$ eV-cm for CdSe.

$$R_{(t)} = \left(\frac{(1 - f_{(t)})\, C_o 3V_m}{4\pi N_{eff}}\right)^{1/3} \qquad \text{and} \quad R_c \equiv \left(\frac{C_o 3V_m}{4\pi N_{eff}}\right)^{1/3} \tag{4-12}$$

$$\lambda_{abs} = \frac{hc}{E_g + X/R} \tag{4-13}$$

If the peak photoluminescence photon emission energy, E_{PL}, is always lower than the 1s–1s absorbance peak energy E_{abs} by an energy shift ($\Delta E_{AP} \sim -0.14$ eV + 0.074 x E_{abs} or $\Delta E_{AP} \sim 0.025$ eV for CdSe quantum dots when 2 eV < E_{abs} < 2.5 eV based on initial experimental observations), then (4-13) can be modified to calculate the wavelength of

the PL peak λ_{PL} (in cm) (4-14). Right when all Cd precursors have been consumed, the average nanocrystal radius reaches the completion radius R_c (4-12), and PL emission occurs at a completion wavelength λ_c (4-14), which marks the knee in a plot of λ_{PL} versus synthesis time.

$$\lambda_{PL} = \frac{hc}{E_g + X/R - \Delta E_{AP}} \qquad \text{and } \lambda_c \equiv \lambda_{PL(R=R_c)} \tag{4-14}$$

Temperature Dependence of Growth Rate

It would be convenient to monitor the molar growth rate and the nanocrystal radius using photoluminescence spectra, because PL peaks form well-defined Gaussian distributions in photon energy. To estimate R, Equation (4-14) is solved for R to obtain (4-15). Theoretically, Arrhenius analysis of redshifts is possible because *v* is proportional to $d\lambda_{PL}/dt$, as will be shown. The bulk Cd concentration decreases from its original level according to (4-16), due to the growth of spherical nanocrystal, if N_{eff} is constant, and if Cd is not consumed by any other mechanism. However, if the reaction yield, *y*, is not 100%, then the actual number of quantum dots N is less than N_{eff}, or $N = y*N_{eff}$. The molar growth rate of each individual quantum dot is proportional to the rate at which C_{bulk} is depleted (4-17). Substituting (4-15) and (4-16) into (4-17) and then differentiating with respect to time yields Equation (4-18). In this case, the experimental $1/R$ photon energy dependence was used instead of the $1/R^2$ dependence from the effective mass approximation; therefore R^4 appears in (4-18) instead of R^5, as published earlier.[69]

$$R = \frac{X}{hc/\lambda_{PL} + \Delta E_{AP} - E_g} \tag{4-15}$$

$$C_{bulk(t)} = C_o - \frac{N_{eff}}{V_{org}} \frac{4\pi R_{(t)}^3}{3V_m} \tag{4-16}$$

$$v = \frac{V_{org}}{N_{eff}} \frac{dC_{bulk}}{dt} \tag{4-17}$$

$$v = \frac{d\lambda_{PL}}{dt} \frac{R^4}{\lambda_{PL}^2} \frac{4\pi hc}{V_m X} \tag{4-18}$$

To the degree that the above assumptions hold, Equation (4-18) is a convenient way to track the QD growth rates by monitoring PL redshift rates. To estimate Q from $d\lambda/dt$, redshift rates at different temperatures could be compared at a common test wavelength. Equation (4-18) shows how fixing λ_{PL} minimizes sensitivity to R, in order to focus on the temperature dependence of v. If the molar growth rate, v, has Arrhenius temperature dependence, then an Arrhenius plot of $\ln\{v\}$ versus $1/T$, would follow a straight line, with the slope, $-Q/k_b$. It may be possible to plot $ln\{d\lambda_{PL}/dt\}$ versus $1000/T$, or to plot $ln\{1/t_c\}$ versus $1000/T$, and get the same activation energy from the slope, $-Q/1000T$.